



Molecular Crystals and Liquid Crystals Incorporating Nonlinear Optics

Publication details, including instructions for authors and
subscription information:

<http://www.tandfonline.com/loi/gmcl17>

Electro-Optic Effects on Liquid Crystalline Polysiloxanes with Negative Dielectric Anisotropy

S. Kohjiya^a, A. Ono^a, T. Kishimoto^a, S. Yamashita^a, H.
Yanased^a & T. Asada^{a b}

^a Department of Material Science, Kyoto Institute of Technology,
Matsugasaki, Kyoto, 606, Japan

^b Department of Polymer Chemistry, Kyoto University, Kyoto,
606, Japan

Version of record first published: 22 Sep 2006.

To cite this article: S. Kohjiya, A. Ono, T. Kishimoto, S. Yamashita, H. Yanased & T. Asada
(1990): Electro-Optic Effects on Liquid Crystalline Polysiloxanes with Negative Dielectric
Anisotropy, *Molecular Crystals and Liquid Crystals Incorporating Nonlinear Optics*, 185:1, 183-197

To link to this article: <http://dx.doi.org/10.1080/00268949008038501>

PLEASE SCROLL DOWN FOR ARTICLE

Full terms and conditions of use: <http://www.tandfonline.com/page/terms-and-conditions>

This article may be used for research, teaching, and private study purposes. Any
substantial or systematic reproduction, redistribution, reselling, loan, sub-licensing,
systematic supply, or distribution in any form to anyone is expressly forbidden.

The publisher does not give any warranty express or implied or make any
representation that the contents will be complete or accurate or up to date. The
accuracy of any instructions, formulae, and drug doses should be independently
verified with primary sources. The publisher shall not be liable for any loss, actions,
claims, proceedings, demand, or costs or damages whatsoever or howsoever caused
arising directly or indirectly in connection with or arising out of the use of this material.

Electro-Optic Effects on Liquid Crystalline Polysiloxanes with Negative Dielectric Anisotropy

S. KOHJIYA, A. ONO, T. KISHIMOTO, S. YAMASHITA, H. YANASE† and T. ASADA†

Department of Material Science, Kyoto Institute of Technology, Matsugasaki, Kyoto 606, Japan

(Received February 2, 1990; in final form April 17, 1990)

Three ester-type low molecular-weight liquid crystals having vinyl groups were synthesized and subjected to hydrosilylation, i.e., the reaction with polysiloxanes carrying hydrosilyl groups using a platinum compound as a catalyst. The thermotropic nature of the resultant liquid crystalline polymers (LCPs) was characterized. The application of the electric field changed the optical transparency of the LCPs. The effects of the applied voltage, the sample thickness and the frequency were studied. The results were explained by the theory developed for low molecular-weight liquid crystals, but a few different behaviors were also recognized. The observed electro-optic effects strongly suggest that the LCPs are not suitable as materials for displays due to slower responses, which are inherent in polymeric liquids.

Keywords: *electro-optic effect, liquid crystal, liquid crystalline polymer, polysiloxane, rise time, decay time*

INTRODUCTION

Liquid crystals (LCs) are now known by their display devices (LCDs),^{1–5} and recently even a television set with LCD has been found in the market.⁶ This usefulness of LCD is based on the electro-optic effects of LC molecules, which have a cylindrical or rod-like molecular architecture.^{1–4,7–10} This geometrical feature is assumed to be the origin of its anisotropies of physical properties such as refractive index, magnetic susceptibility and dielectric constant, to name a few. Hence, the optical state of LC molecules is affected by the magnetic field as well as by the electric field.

In this paper the properties of liquid crystalline polymers (LCPs) based on poly(siloxane) are reported. They may prove to be useful as functional materials in electronic technology, especially electro-optic applications being in our minds. There are two configurations for LCPs, main-chain type and side-chain type. Main-

†Department of Polymer Chemistry, Kyoto University, Kyoto 606, Japan

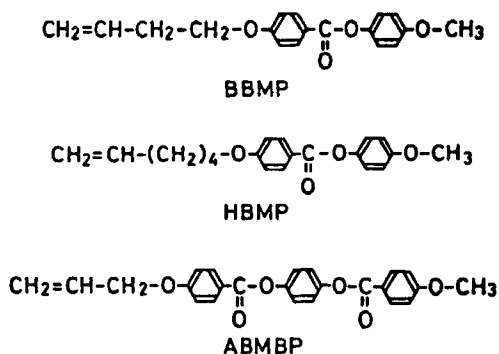


FIGURE 1 Monomeric mesogens (low molecular-weight LCs) used in the present study.

chain type LCPs, especially aromatic polyester derivatives, are among engineering plastics of high modulus, because the macromolecular chains can be oriented in a liquid crystalline state.¹¹

Side-chain type LCPs, however, must be much better than the main-chain type for the alignment of mesogenic groups responding to the applied field, since the mesogenic groups are bonded only at one end.^{12–14} In order to achieve an easy alignment of the mesogens, we have chosen poly(siloxane)s as a polymeric main chain. Poly(siloxane)s show their glass-transition temperature (T_g) at well below -100°C ,¹⁵ which must be the result of their active microbrownian segmental motions. In fact, poly(siloxane)s are well known for their versatility at low temperatures among elastomers.

It is fascinating to chemically combine anisotropic liquid (LC) with isotropic solid (amorphous polysiloxane). As LC molecules (mesogen) we have synthesized three compounds, shown in Figure 1. They are chosen because they are very stable, unlike azomethine compounds, which are susceptible to hydrolysis by moisture. Among the three compounds, the syntheses of BBMB and HBMB (see Figure 1) were already reported.^{12,16} ABMBP is reported first in this communication as far as we are aware. These three compounds are chemically bonded to poly(siloxane)s by a hydrosilylation reaction. The resultant polymeric liquid crystals are subject to characterizations and electro-optic measurements.

THEORETICAL BACKGROUND

The mesogenic groups that we have synthesized contain carbonyl groups. This group carries the largest dipole moment in these molecules and is perpendicular to the molecular long axis (see Figure 1). We assume therefore that the three compounds have dielectric constants of negative anisotropy, i.e.,

$$\epsilon' = \epsilon_{\parallel} - \epsilon_{\perp} < 0 \quad (1)$$

where ϵ is the dielectric constant, \parallel and \perp mean parallel and perpendicular to the molecular axis, respectively. Theoretical treatments on the hydrodynamic instability phenomena of negative anisotropic molecules are well established.⁴

Under the application of a direct current (dc) electric field or an alternating current (ac) field of a lower frequency than the cut-off frequency (f_c), the Williams domain is observed when the voltage exceeds a threshold value (V_c), and a dynamic scattering mode (DSM) following at a higher voltage. V_c and f_c are given as follows^{4,17-19}

$$V_c^2 = \left(\frac{E_z \lambda d}{2} \right)^2 = \frac{V_0^2}{\zeta^2 - 1} \quad (2)$$

$$V^2 = \pi^2 c^2 K \epsilon_{\parallel} / \epsilon_{\perp} (\epsilon_{\perp} - \epsilon_{\parallel}) \quad (3)$$

$$\zeta^2 = \left(\frac{\epsilon_{\parallel} k}{\epsilon \eta} - 1 \right) \left(\frac{\sigma_{\perp} \epsilon_{\parallel}}{\sigma_{\parallel} \epsilon_{\perp}} - 1 \right) \quad (4)$$

$$f_c = (\zeta^2 - 1)^{1/2} / 2\pi\tau \quad (5)$$

$$\tau = \epsilon_{\parallel} / \sigma_{\parallel} \quad (6)$$

where E_z is the z component of the applied field, $d/2$ is the thickness of the cell containing LC, c and k are the constants, K is the elastic constant, η is viscosity, σ is electrical conductivity, ζ and τ are the Helrich parameter¹⁸ and dielectric relaxation time, respectively.

Under a higher frequency field than f_c , the movement of space charge originated from dielectric anisotropy can not follow the polarity change of the electric field. Therefore, the hydrodynamic instability phenomena in this region are called those in the dielectric regime. On the other hand, the region described previously is called the conducting regime. In the dielectric regime the alignment of mesogenic molecules changes by the application of field, and the threshold voltage is given as follows⁴

$$V_F = \sqrt{\frac{K}{\Delta\epsilon}} \pi \quad (7)$$

The reorientation of anisotropic molecules by the electric field results in the changes in their optical properties, i.e., refractive index, hence reflectance or transparency. The effect is called the electro-optic effect.

The LC cell is a kind of capacitance. On the application of electric field, the dielectrics are forced to orient according to the field. However, it takes time for

LC molecules to reorient. This delay is given as the rise time (τ_R)^{4,20,21}

$$\tau_R = \frac{\eta d^2}{\Delta\epsilon V^2 - \pi^2 K} \quad (8)$$

$$\Delta\epsilon = \epsilon_{\perp} - \epsilon_{\parallel} \quad (9)$$

where d is a cell thickness and V is the applied voltage. Note that the definition of $\Delta\epsilon$ is different from Equation (1). $\Delta\epsilon$ in Equation (9) is positive for the present mesogens. The inverse of Equation (8) gives

$$\tau_R^{-1} = \frac{1}{d^2} \left(\frac{\Delta\epsilon}{\eta} V^2 - \frac{K}{\eta} \pi^2 \right) \quad (10)$$

This equation gives the dependency of τ_R^{-1} on V^2 .

On the other hand, the decay time (τ_D), which is the time required for LC molecules to go back to the original state after the turn-off of the field, is not dependent on the voltage. τ_D is expressed as^{4,12}

$$\tau_D = \frac{\eta d^2}{\pi^2 K} \quad (11)$$

In this paper, the rise time (τ_R) and the decay time (τ_D) are determined, because these values are very important electro-optic parameters in order to evaluate materials for electro-optical applications.

EXPERIMENTAL

Materials

The synthetic routes of the three mesogenic molecules are shown in Figure 2. They are aromatic esters and chemically very stable, which means that the handling of them is very easy. They have carbon-carbon double bonds to afford the site for chemical bonding to polysiloxanes having silicon-hydrogen bonds. As matrix polymers to be combined with the mesogenic compounds, three poly(siloxane)s were used; poly(methyl hydrogen siloxane) (PS 100), and two copolymers of methyl-hydrogen-siloxane units and dimethylsiloxane units whose methyl-hydrogen-siloxane-units contents were 32 mole % (PS 30) and 13.5 mol % (PS 13).

The hydrosilylation reaction of the mesogens having double bonds were carried out in toluene using hexachloroplatinic acid as a catalyst (see Figure 3). Eight polysiloxanes having three kinds of mesogenic groups, i.e., the liquid crystalline polymers (LCPs) employed in this work, were prepared following the procedures shown in Figures 2 and 3. The compositions of the LCPs are shown in Table I.

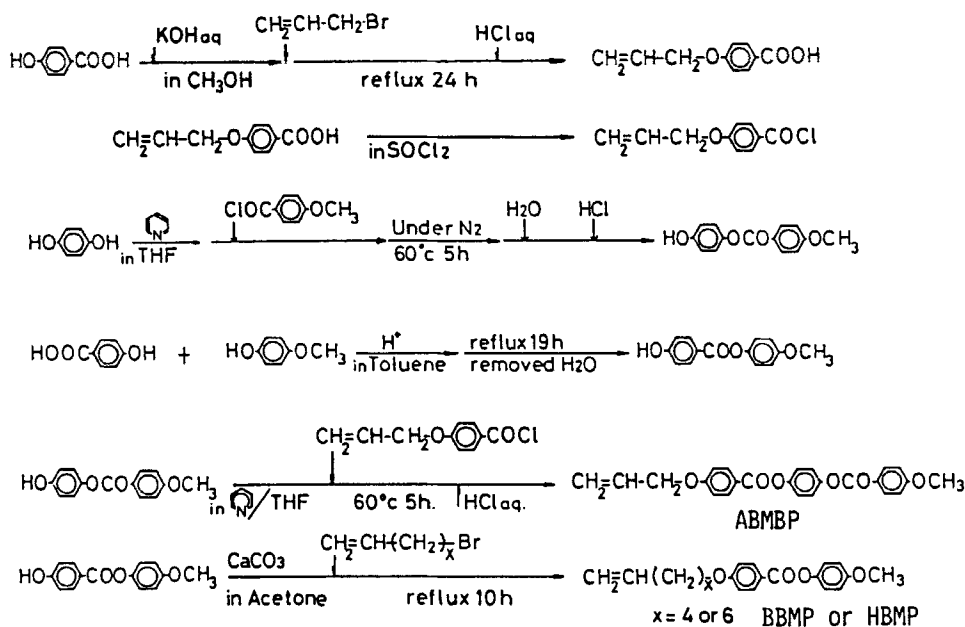


FIGURE 2 Synthetic routes of monomeric mesogens.

Analyses

All the materials were identified by infrared and proton nuclear magnetic resonance spectroscopies for their chemical structures, and gel-permeation chromatography.²² Differential scanning calorimetry (DSC) measurements were carried out on DSC-20 (Seiko Electronics Co.). The sample amount was 10 mg, and the heating rate was 10°C/min.

Electro-Optic Measurement

The block diagram of the apparatus for electro-optic measurements is shown in Figure 4. The light from a halogen lamp (light source, LS) passed through the filter

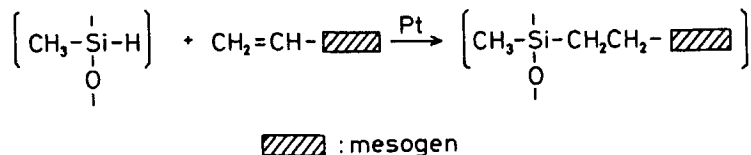


FIGURE 3 Reaction of monomeric mesogen with poly(methyl hydrogen siloxane)-hydrosilylation with Pt catalyst.

TABLE I
Chemical compositions of LCPs

Sample code	polysiloxane	mesogen (mol%) ^{a)}		
	Si-H units (mol%)	BBMP	HBMP	ABMBP
BB-PS 30	32	30	-	-
BB-PS 100	100	100	-	-
HB-PS 30	32	-	30	-
HB-PS 100	100	-	100	-
ATB-PS 13	13	-	-	13
ATB-PS 30	32	-	-	30
BcoA-PS 100	100	70	-	30
HcoA-PS 100	100	-	70	30

^{a)} If the total mol% of mesogens is below 100, the rest is the mol% of dimethylsiloxane units.

(f), a polarizer (P) and a sample cell (C) placed on a hot stage (HS). The construction of C: the sample was sandwiched in two electro-conductive glass (Nesa[®] glass) plates with a spacer (FEP film) of a prescribed thickness. The glass plates were used after washing the surfaces by acetone and distilled water. No special treatments were carried out for the alignment. The light which came out of the cell went through an analyzer (A, crossed with P) and divided into two; one for visual observation or video camera (VC), the other to photo diode (PD) for the

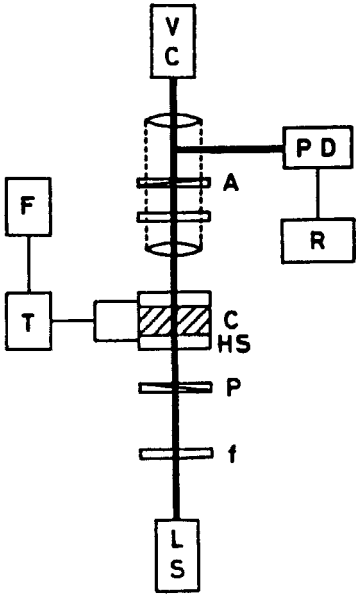


FIGURE 4 Apparatus for electro-optic measurement.

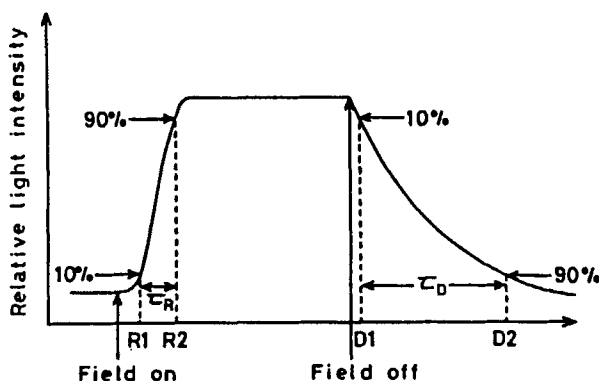


FIGURE 5 Schematic depiction of recorder traces and the definitions of τ_R and τ_D .

recording (R) of the light intensity. An electric field was applied to the sample from the function generator (F) through a transformer (T).

In Figure 5 a schematic depiction of the result that we obtained is displayed. Definitions of the rise time (τ_R) and the decay time (τ_D) are indicated in the Figure.

RESULTS AND DISCUSSION

Thermotropic Nature

Table II shows the thermotropic liquid crystalline properties of the three mesogens. The melting temperature (T_m) and the clearing temperature (T_c), were determined by DSC. Here, T_c is the transition point from anisotropic liquid (LC) to isotropic liquid. The textures were found to be the Shlieren type by optical observations on a polarized light microscope. Similar results were obtained on LCPs, and DSC

TABLE II
Phase transition temperatures of low molecular-weight
liquid crystals measured by DSC

Sample code ^{a)}	T_m ^{b)} (°C)	T_c ^{c)} (°C)	Mesophase
BBMP	41.0	73.0	nematic
HBMP	59.0	63.0	nematic
ABMBP	154.5	249.0	nematic

a) See Figure 2.

b) Melting temperature.

c) Clearing temperature where the anisotropic liquid becomes isotropic.

TABLE III
Phase transition temperatures of LCPs by DSC

Sample code ^{a)}	T _g ^{b)} (°C)	T _m (°C)	T _c (°C)	Mesophase
BB-PS 30	-30.0	- ^{c)}	-	nematic
BB-PS 100	-2.0	-	75.5	nematic
HB-PS 30	-38.0	-	32.0	nematic
HB-PS 100	-6.0	-	87.5	nematic
ATB-PS 13	-	69.0	133.0	nematic
ATB-PS 30	-	67.5	152.0	nematic
ATB-PS 100	-	74.0	242.0 ^{d)}	nematic
BcoA-PS 100	19.5	-	162.0	nematic
HcoA-PS 100	11.5	-	147.0	nematic

a) See Table 1.

b) Glass-transition temperature.

c) Not clear on DSC, but a little higher than room temperature.

d) From optical observation on a polarized microscope.

results are shown in Table III. From the comparison of Tables II and III, the most interesting point is the widening of the mesomorphic temperature range (MR) by the incorporation of mesogens onto polysiloxanes as side chains. This point is illustrated in Figures 6 and 7. MR is defined as the temperature range between T_m and T_c or between T_g and T_c . From the Figures you can recognize drastic increases of MR for both HB-PS and ATB-PS. This phenomenon was already reported by Finkelman *et al.*,^{12,13,16} and our observations reconfirmed their results. However,

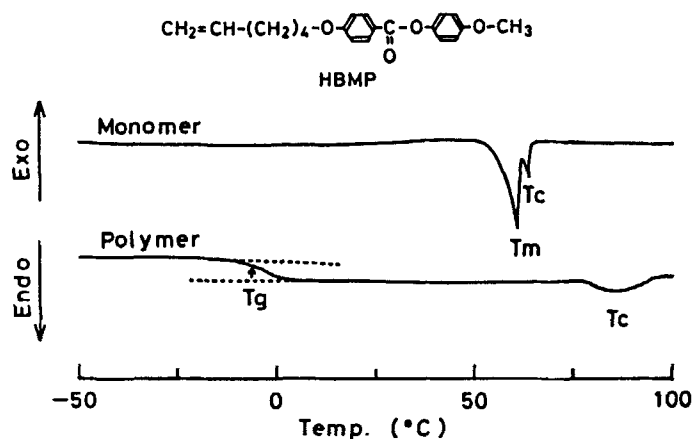


FIGURE 6 DSC traces of HBMP and HB-PS 100.

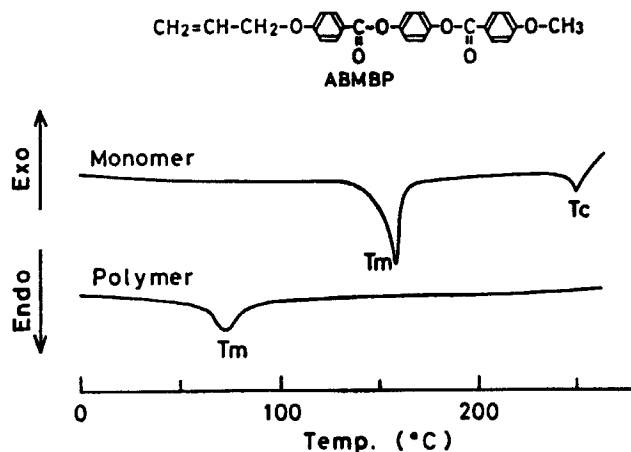


FIGURE 7 DSC traces of ABMBP and ATB-PS 100.

our results seem to be more drastic than theirs, and the exact reason for this phenomenon is still to be elucidated.

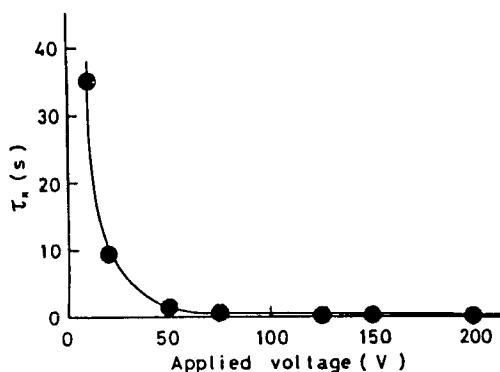
The second point that should be mentioned is T_g or T_m of LCPs. In case of BB-PS or HB-PS, T_m was not found. Glass transitions were observed between T_m of monomeric LCs and T_g of polysiloxane (ca. -140°C). On the other hand, T_m was observed on LCPs from ABMBP, although the temperatures were much lower than that of ABMBP itself. Because ABMBP has three phenylene rings connected by an ester linkage, it possesses a much stronger liquid crystalline character than BBMP or HBMP. This is the reason why T_m appeared in LCPs from ABMBP, while only T_g was observed in LCPs from BBMP and HBMP.

The textures of all the samples were the Schlieren type, which enabled us to assign the mesophases to the nematic state.^{1,23} The textures of monomeric LCs were also nematic. Probably due to higher viscosity, the textures of LCPs were finer than those of monomeric LCs under equivalent conditions.

Electro-Optic Effect: Influences of Voltage and Sample Thickness

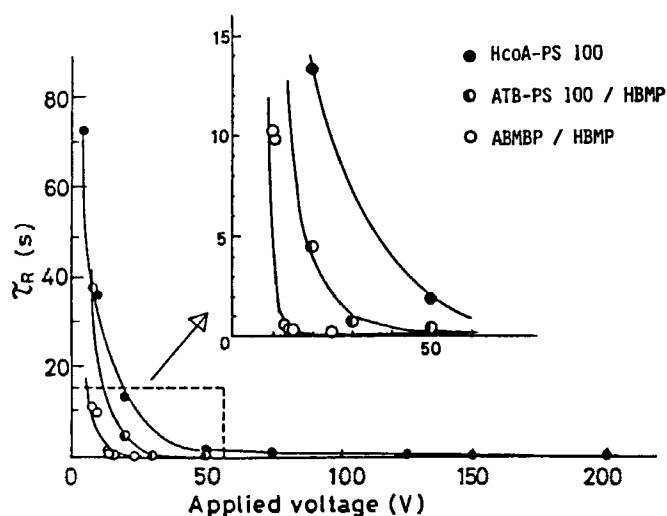
When an electric field was applied, the cell became brighter under crossed polarizers. This change of light intensity was recorded, and τ_R and τ_D were determined. Here, the frequency of alternating current was 2 kHz, which we assumed to be much higher than f_c (see Equation (5) and the later discussion on the frequency effect).

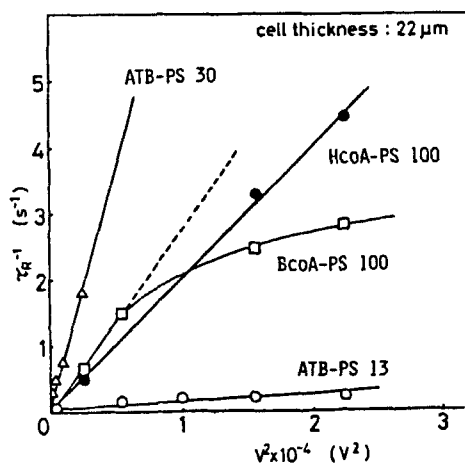
Figures 8 and 9 show the effect of voltage at 2 kHz on the τ_{RS} of BcoA-PS 100 and HcoA-PS 100, respectively. It is to be noted that the temperature was kept at 90% of T_c by the absolute temperature. With the increase of voltage, the rise time decreased rapidly until the voltage of ca. 50 V. Even above 50 V, τ_R decreased with the increase of voltage, but the slope was much smaller than below 50 V. Above 100 V, the rise time was ca. 200 ms. Cole and Simons reported almost the same τ_R for LCP with a positive dielectric anisotropy.²⁵⁻²⁸ 200 ms seems to be the

FIGURE 8 Applied voltage dependency of τ_R for BcoA-PS 100.

lowest value as the response time of LCPs prepared from poly(siloxane)s. In Figure 9 the results on ATB-PS 100/HBMP and ABMBP/HBMP mixtures were also included. It is evident that the mixing of a low molecular-weight mesogen considerably decreased the viscosity, hence the decrease of τ_R (Equation (10)).

The results so far are replotted in Figure 10 according to Equation (10), together with the results on ATB-PS 13 and ATB-PS 30. The linear correlations were observed except BcoA-PS 100 which deviated from the linearity in the higher voltage zone. It can be said that Equation (8) holds in LCPs as well as in low molecular-weight LCs.^{4,19,24} This relationship had also been observed on poly(methacrylate) derivatives having a positive anisotropy.¹⁴ From the slope and the intercept in Figure 10, $\Delta\epsilon/\eta$ and K/η were calculated, respectively. V_F values

FIGURE 9 Applied voltage dependencies of τ_R s for HcoA-PS 100, ATB-PS 100/HBMP blend and ABMBP/HBMP blend.

FIGURE 10 τ_R^{-1} vs. V^2 plot according to Equation (10).

can be evaluated from these values using Equation (7). The results will be tabulated later.

The influence of the sample thickness is shown in Figure 11. The linearity of Equation (10) was also found in this Figure. Equation (8) claims a linear relation between τ_R and d^2 , which was also found to be the case, although the plots were not shown here. The V_F values so far obtained are listed in Table IV. According to Equation (7) V_F does not depend on d (the sample thickness), but V_F of HcoA-PS 100 changed almost linearly with d . This phenomenon is to be explained by the properties of the LCPs. The mesogens are completely compatibilized with polymer

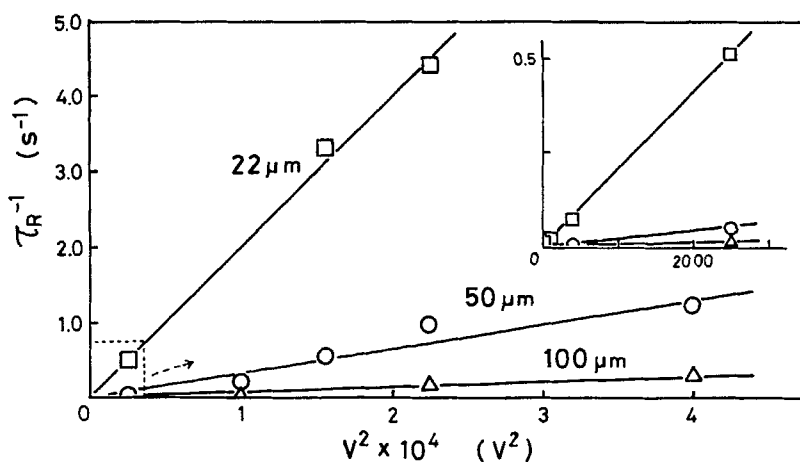
FIGURE 11 τ_R^{-1} vs. V^2 plot; effect of sample cell thickness.

TABLE IV
The threshold voltage $V_F^{a)}$ from the voltage dependency of $\tau_R^{b)}$

Sample code	BcoA-PS 100		HcoA-PS 100		ATB-PS 13	ATB-PS 30
Sample thickness (μm)	22	22	50	100	22	22
$V_F^{a)}$ (V)	4.30	5.72	13.2	34.7	165	36.8

a) See Equation (7).
b) See Equations (8) and (10).

chains, because they are chemically bonded. When we disregard the bonding, the mesogens are assumed to be in a polymeric liquid, i.e., in a viscous solution. The solvent in this case is poly(siloxane), which is a relatively non-polar medium. This macromolecular medium necessitated the higher voltages for the alignment of mesogens when the sample thickness became larger, because the field effect is due to a transmission of the torque from one LC molecule to another, i.e., a kind of co-operativity among LC molecules. This explanation may also be adequate for the larger τ_R of ATB-PS 15 than that of ATB-PS 30. The concentration of the mesogen (ABMBP) was higher in ATB-PS 30.

As is expressed in Equation (11), τ_D did not depend on the applied voltage (see Figure 12). This Figure also reveals the much larger τ_D of LCP than those of low

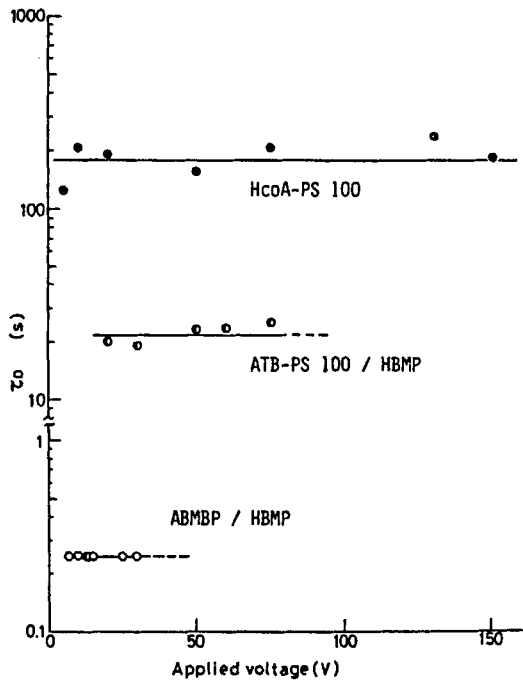


FIGURE 12 τ_D vs. V plot; effect of monomeric mesogen blending.

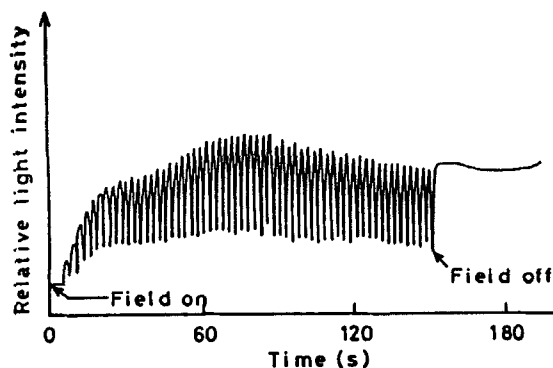


FIGURE 13 Electro-optic effect at low ac frequency (0.2 Hz) of HcoA-PS 100.

molecular-weight LCs. In the decay process there is no operating of outside forces for the mesogens to reorient. Therefore, the difference of viscosity was directly effective as seen in Equation (11).

Electro-Optic Effect: Influence of Frequency.

Previously, we assumed that 2 kHz was a much higher frequency than the cut-off frequency (f_c). To elucidate the nature of the electric field effect, the frequency effect is very important. We carried out some preliminary experiments on this effect, which are described now.

In Figure 13 is shown the recorder trace under the electric field of 0.2 Hz. The voltage was 50 V. No change was observed for ca. 5 s at the initial stage. This observation indicates that the cell containing LCP is a capacitor.^{4,13} After 5 s or so, the light intensity increased with dark-bright cycles. This cyclic change of light intensity is in accordance with the change of electric polarity, which clearly suggests that the alignment of mesogens follows the change of ac voltage. Therefore, 0.2 Hz is well below f_c and 50 V is below V_c . However, if ionic or some electro-conducting impurities are present, V_c can be below this voltage and DSM may be observed, because the present mesogens all have negative anisotropy in their dielectric constants.^{4,17}

Not always but in many cases, the LCP did not return to the original state when low frequency fields were applied. In other words, τ_D was very large, and the domain texture was preserved. The same phenomenon was also reported by Cole *et al.*,^{25–28} and might enable us to consider the present materials to be of use for memory or data storage devices.

Figure 14 shows the effect of frequency on τ_R . Because the mesogens followed the movement of the field at very low frequencies, τ_R decreased with the increase of frequency. At around 100 Hz, it became impossible for them to follow the field. The larger frequency resulted in much larger τ_R . The electro-optic effect that we observed above ca. 100 Hz seems to be the hydrodynamic instability phenomena at the dielectric regime, and the dynamically-induced dielectric anisotropy might

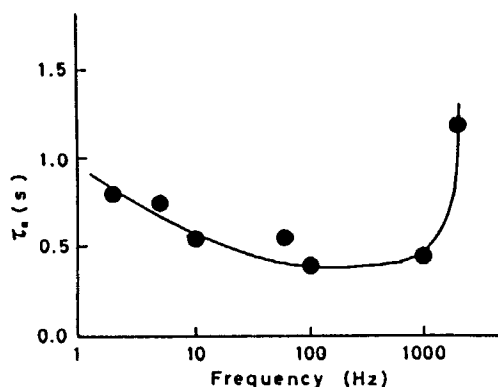


FIGURE 14 AC frequency dependence of τ_R of HcoA-PS 100.

become effective. This effect seems to decrease the $\Delta\epsilon$, which resulted in a slower response at higher frequencies.

Alignment of the Mesogens

By the application of the electric field, the present LCPs always became brighter under crossed polarizers. We assumed that the mesogens initially aligned in a homeotropic state and the orientation of the dipoles under the electric field resulted in movement towards the homogeneous alignment. This assumption explains our results reasonably, and the initial homeotropic alignment on the glass plate was confirmed by conoscopic observations.

The driving force for the initial homeotropic orientation of the present LCPs is a very interesting point that demands further study. We tentatively assume that the poly(siloxane) chains in the LCPs may be adhered first on the glass surfaces. Because mesogens were grafted onto those chains, the homeotropic orientation was thermodynamically more stable for the mesogens. However, the adhesion between the polymer and the glass surface may not be strong enough to resist the influence of the electric field.

Studies on the exact picture on the alignment of poly(siloxane)-based LCP on the glass are in progress, which seems to be most interesting not only from a scientific viewpoint but also from an industrial one.

References

1. G. W. Gray and P. A. Winsor, "Liquid Crystals and Plastic Crystals" John Wiley & Sons (New York, 1974).
2. A. Ciferri, W. R. Krigbaum and R. B. Meyer eds., "Polymer Liquid Crystals" Academic Press (New York, 1982).
3. L. L. Chapoy ed., "Recent Advances in Liquid Crystalline Polymers" Elsevier Applied Science (London, 1985).
4. A. Sasaki ed., "Fundamentals and Applications of Electronics on Liquid Crystals" Ohm Sha (Tokyo, 1979, in Japanese).

5. G. H. Brown and P. P. Crooker, *Chem. & Eng. News*, 1983, Jan. 31, p. 24.
6. Nikkei New Materials, 1986, no. 22, p. 33 (in Japanese).
7. P. J. Flory, in Reference 2, Chapter 4.
8. P. G. de Gennes, in Reference 2, Chapter 5.
9. P. J. Flory, in Reference 3, Chapter 6.
10. M. Doi and N. Kuzuu, *J. Appl. Polym. Sci.: Appl. Polym. Symp.* **41**, 65 (1985).
11. D. C. Prevorsek, in Reference 2, Chapter 12.
12. H. Finkelmann, in Reference 2, Chapter 2.
13. H. Finkelmann and G. Rehage, *Adv. Polym. Sci.*, **60/61**, 99 (1984).
14. V. P. Shibaev and N. A. Plate, *Adv. Polym. Sci.*, **60/61**, 173 (1984).
15. W. Lynch, "Handbook of Silicone Rubber Fabrication" Van Nostrand Reinhold (New York, 1978).
16. H. Finkelmann and G. Rehage, *Makromol. Chem. Rapid Commun.*, **1**, 31 (1980); N. A. Apfel, H. Finkelmann, G. M. Janini, R. J. Raub, B.-H. Luhman, A. Price, W. L. Roberts, T. J. Shaw and C. A. Smith, *Anal. Chem.*, **57**, 651 (1985).
17. E. F. Carr, *J. Mol. Cryst.*, **7**, (1969).
18. W. J. Helfrich, *J. Chem. Phys.*, **51**, 4092 (1969).
19. W. R. Krigbaum, in Reference 2, Chapter 10.
20. H. Koelmans and A. M. Van Boxtel, *Mol. Cryst. Liq. Cryst.*, **12**, 185 (1971).
21. E. Jackman and E. P. Raynes, *Phys. Lett.*, **39A**, 69 (1972).
22. S. Kohjiya, A. Ono and S. Yamashita, Nippon Gomu Kyokaishi (in Japanese), to be published.
23. D. Demus and L. Richter, "Textures of Liquid Crystals" Verlag Chemie (Weinheim, 1978).
24. W. R. Krigbaum, *J. Appl. Polym. Sci.: Appl. Polym. Symp.*, **41**, 149 (1985).
25. A. I. Hopwood and H. J. Coles, *Polymer*, **26**, 1312 (1985).
26. M. S. Sefton and H. J. Coles, *Polymer*, **26**, 1319 (1985).
27. H. J. Coles, Faraday Discussion, *Chem. Soc.*, **79**, 201 (1985).
28. R. Simons and H. J. Coles, *Polymer*, **27**, 811 (1986).